Bandemehr, Jascha; Stoll, Christiane; Heymann, Gunter; Ivlev, Sergei I.; Karttunen, Antti J.; Conrad, Matthias; Huppertz, Hubert; Kraus, Florian

The Crystal Structure of MnF3 Revisited

Published in:
Zeitschrift fur Anorganische und Allgemeine Chemie

DOI:
10.1002/zaac.202000025

Published: 15/07/2020

Document Version
Publisher's PDF, also known as Version of record

Journal of Inorganic and General Chemistry
ZAAC
Zeitschrift für anorganische und allgemeine Chemie
DOI: 10.1002/zaac.202000025
ARTICLE

The Crystal Structure of MnF_3 Revisited

Jascha Bandemehr,[a] Christiane Stoll,[b] Gunter Heymann,[b] Sergei I. Ivlev,[a] Antti J. Karttunen,[c] Matthias Conrad,[a] Hubert Huppertz,[b] and Florian Kraus*[a]

Dedicated to Professor Manfred Scheer on the Occasion of his 65th Birthday

Abstract. We correct the crystal structure of MnF_3, of which the space group was reported as monoclinic *C*2/*c* (no. 15) with *a* = 8.9202, *b* = 5.0472, *c* = 13.4748 Å, *β* = 92.64°, *V* = 606.02 Å^3, *Z* = 12, *mS*48, *T* not given, likely 298 K. In the structure model proposed here, we use a unit cell of one third of the former volume. The ruby red crystals of MnF_3 were synthesized by a high-pressure/high-temperature method, where MnF_4 was used as a starting material. As determined on a single crystal, MnF_3 crystallizes in the monoclinic space group *I*2/*a* (no. 15) with *a* = 5.4964(11), *b* = 5.0084(10), *c* = 7.2411(14) Å, *β* = 93.00(3)°, *V* = 199.06(7) Å^3, *Z* = 4, *mS*16, *T* = 183(2) K. The crystal structure of MnF_3 is related by a direct group-subgroup transition to the VF_3 structure-type. We performed quantum chemical calculations on the crystal structure to allow the assignment of bands of the obtained vibrational spectra.

Introduction

Manganese(III) fluoride is a ruby red colored compound, which was first mentioned in 1867.[1] The first positive proof that pure MnF_3 was synthesized was given in 1900 from *Moissan*.[2] It can be prepared by fluorination of MnI_2, MnF_2, or $(NH_4)_2MnF_5$ at 250 °C.[2–4] In 1957, *Hepworth* and *Jack* published some details about the crystal structure.[5,6] From powder X-ray data they could deduce a monoclinic cell in space group *C*2/*c*, which contained twelve Mn and 36 F atoms. Additionally, they reported the coordinates of all atoms. In 1993, *Schrötter* and *Müller* reacted a prefluorinated mixture of SmF_3 and NH_4MnF_3 at 250 °C in an autoclave filled with 100 % F_2 at 200 bar. The obtained violet product was sealed in a gold ampoule and heated up to 650 °C for 21–28 days and cooled down with 40 K per day. The ruby red crystals of MnF_3 were collected and the crystal structure was determined on the basis of the previously described one.[7] According to *Müller* and co-worker, MnF_3 crystallizes with twelve formula units in the unit cell (*a* = 8.9202, *b* = 5.0472, *c* = 13.4748 Å, *β* = 92.64°, *V* = 606.02 Å^3, *Z* = 12, *mS*48, *T* likely 298 K) with two crystallographically independent manganese and five independent fluorine atoms.[7] Both Mn atoms were coordinated by six fluorine atoms in shapes of distorted octahedra due to the Jahn–Teller effect as the electron configuration of the Mn^{3+} cations is [Ar]3*d*^{4}. The coordination octahedra were connected through corners to each other and built a three-dimensional network.

We serendipitously obtained single crystals of MnF_3 by a high-pressure/high-temperature method, however observed a unit cell volume of only one third of the previously reported one.[5–7] Here, we present the crystal structure of MnF_3 containing only one symmetry independent Mn and only two symmetry independent F atoms.

Results and Discussion

We synthesized MnF_3 by compressing MnF_4, on which we will report in the near future,[8] inside a platinum capsule using a multi-anvil press (for details see Experimental Section). Likely, MnF_4 decomposed thermally[9] to MnF_3 due to the reaction temperature of 500 °C and the released fluorine reacted with the capsule. We obtained ruby red single crystals of MnF_3 beside ruby red powder (see Figure 1) and determined the crystal structure from X-ray diffraction data.

Crystal Structure

The volume of our unit cell is with 199.06(7) Å^3 approximately three times smaller than the previously reported one of 606.02 Å^3.[5–7] The lattice parameters determined on a single crystal are *a* = 5.4964(11), *b* = 5.0084(10), *c* = 7.2411(14) Å, *β* = 93.00(3)°, *V* = 199.06(7) Å^3, *Z* = 4, *mS*16, *T* = 183(2) K. Details of the structure solution and refinement are given in Table 1 and the atomic coordinates are given in Table 2. Seven crystallographically independent atoms were required in the previous structure model, whereas in ours only three symmetry independent atoms are necessary (Table 2).

* Prof. Dr. F. Kraus
E-Mail: f.kraus@uni-marburg.de
[a] Fachbereich Chemie
Philipps-Universität Marburg
Hans-Meerwein-Str. 4
35032 Marburg, Germany
[b] Institut für Allgemeine, Anorganische und Theoretische Chemie
Universität Innsbruck
Innrain 80–82
6020 Innsbruck, Austria
[c] Department of Chemistry and Materials Science
Aalto University
00076 Aalto, Finland

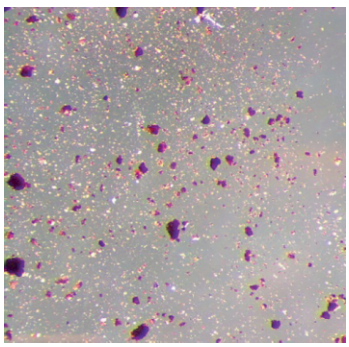

Figure 1. Picture of ruby-red crystals and powder of MnF_3 under a visible light microscope.

Table 1. Selected crystallographic data and details of the structure determination of MnF_3.

Formula	MnF_3
Molar mass /g·mol^{-1}	111.94
Space group (no.)	*I*2/*a* (15)
a /Å	5.4964(11)
b /Å	5.0084(10)
c /Å	7.2411(14)
β /°	93.00(3)
V /Å^3	199.06(7)
Z	4
Pearson symbol	*mS*16
$\rho_{calcd.}$ /g·cm^{-3}	3.735
μ /mm^{-1}	6.379
Color	ruby red
Crystal appearance	block
Crystal size /mm^3	0.03 × 0.03 × 0.02
T /K	183(2)
λ /Å	0.71073 (Mo-K_α)
No. of reflections	2863
θ range /°	4.951–41.267
Range of Miller indices	$-10 \le h \le 9$ $-9 \le k \le 9$ $-13 \le l \le 9$
Absorption correction	multi-scan
T_{max}, T_{min}	0.7481, 0.6528
R_{int}, R_σ	0.0176, 0.0199
Completeness of the data set	0.994
No. of unique reflections	669
No. of parameters	22
No. of restrains	0
No. of constrains	0
S (all data)	1.101
$R(F)$ [$I \ge 2\sigma(I)$, all data]	0.0182, 0.0196
$wR(F^2)$ [$I \ge 2\sigma(I)$, all data]	0.0457, 0.0464
Extinction coefficient	0.039(4)
$\Delta\rho_{max}$, $\Delta\rho_{min}$ /e·Å^{-3}	0.816, –0.716

Table 2. Atomic coordinates and equivalent isotropic displacement parameters U_{iso} for MnF_3.

Atom	Position	*x*	*y*	*z*	U_{iso} /Å^2
Mn(1)	4*d*	1/4	1/4	1/4	0.00370(6)
F(1)	4*e*	1/4	0.13238(15)	0	0.00824(12)
F(2)	8*f*	0.92805(9)	0.45972(11)	0.19290(7)	0.00797(9)

The previous crystal structure can be transformed from *mC* to *mI* via the basis transformation $\boldsymbol{a}_I = -1/3\ \boldsymbol{a}_c + 1/3\ \boldsymbol{c}_c$, $\boldsymbol{b}_I = \boldsymbol{b}_c$, $\boldsymbol{c}_I = -2/3\ \boldsymbol{a}_c - 1/3\ \boldsymbol{c}_c$ and an origin shift of +1/4 for *x*, *y*, and *z* (the indices *I* and *c* correspond to the *mI* and *mC* unit cells, respectively). A comparison of atomic coordinates of the previous crystal structure before and after transformation to *mI* is shown in Table 3. The lattice parameters after transformation are $a_I = 5.4996$, $b_I = 5.0472$, $c_I = 7.2855$ Å, $\beta_I = 92.69°$ and are comparable to the lattice parameters determined on the single crystal.

Comparing the atomic coordinates of the previous structure model (Table 3) with those of the new structure model proposed here (Table 2), one recognizes that the previous Mn(1) and Mn(2) atoms are superimposed by the lattice transformation. Also, the atomic coordinates of the previous atoms F(1) and F(5), as well as those of F(2), F(3), and F(4) become alike and correspond to the atoms F(1) and F(2) of the new structure model, respectively. It is interesting to note that this relation has already been recognized by *Hepworth* and *Jack*[5] and it is unclear why neither they, nor the later report on the single crystal structure, used the smaller unit cell for the structure description.[7] Thus, the crystal structure of MnF_3 is best described with only three symmetry independent atoms in the smaller *mI* unit cell instead of seven in the larger *mC* unit cell.

In the crystal structure of MnF_3, the Mn(1) atom is surrounded by six fluorine atoms in an octahedron-like shape (Figure 2). The Mn–F distances are $2 \times 1.8124(6)$ Å [Mn(1)–F(2)], $2 \times 1.9037(4)$ Å [Mn(1)–F(1)], and $2 \times 2.0806(6)$ Å [Mn(1)–F(2)] and are given in Table 4. The Mn–F distances are comparable to those reported by *Hepworth* and *Jack* (1.79, 1.91, 2.09 Å) as well as those by *Schrötter* and *Müller* (1.8173, 1.9124, 2.0878 Å).[5,7] The distortion of the coordination polyhedron around the Mn atom from O_h symmetry may be explained with the Jahn–Teller effect due to the [Ar]3d^4 electronic configuration of the Mn^{3+} ion. The distorted octahedron is vertex-linked to six other MnF_6 octahedra so that all fluorine atoms are coordinated by two Mn atoms. Thus, a three-dimensional network results, which can be described with the Niggli formula $^3_\infty[MnF_{6/2}]$. The crystal structure can be derived from the VF_3 structure-type as shown in the *Bärnighausen*-tree in Figure 3.

For comparison with the previously reported Coulomb component of the lattice energy of the previous MnF_3 structure model, we carried out MAPLE calculations. The Madelung constant of the current structure model is 8.4054 compared with 8.3311 for the previous one.[7] The Coulomb component of the lattice energy is now 6442 kJ·mol^{-1} and, as may be expected, quite similar to the previously obtained 6437 kJ·mol^{-1}.[7] The Coulomb energy is in good agreement with the result (6427 kJ·mol^{-1}) obtained from the calculated lattice energies of $NaMnF_4$ (7474 kJ·mol^{-1}) and NaF (1047 kJ·mol^{-1}) and deviates only 0.2 %.[11,12] Table 5 lists the motifs of mutual adjunction, effective coordination numbers (ECoN), mean fictive ionic radii (MEFIR), and the calculated charge distribution. Due to the Jahn–Teller distortion and the relatively large Mn(1)–F(2) distance of 2.0806(6) Å, the ECoN values for these two atoms differ slightly from the above described coordination number. The CHARDI calculations show a charge of approximately –1 for the fluorine atoms and, as expected, +3

Table 3. Transformation of the atom positions from *mC* to *mI* for the previously reported crystal structure of MnF_3.[7]

	mC			*mI*			Respective atom in our structure
Mn(1)	0	0	0	¼	¼	¼	Mn(1)
Mn(2)	0.1671	0.5010	0.3340	0.7510	0.7510	–0.2512	Mn(1), (½ + *x*, ½ + *y*, –½ + *z*)
F(1)	0.1667	0.1053	0.5866	1.2566	0.3554	–0.5034	F(1), (3/2 – *x*, ½ – *y*, –½ – *z*)
F(2)	0.3069	0.7156	0.2448	0.4327	0.9656	–0.3017	F(2), (–½ + *x*, ½ + *y*, –½ + *z*)
F(3)	0.4746	0.2075	0.5777	0.9309	0.4575	–0.8024	F(2), (*x*, *y*, –1 + *z*)
F(4)	0.1472	0.2130	0.9119	1.9266	0.4631	–0.8092	F(2), (1 + *x*, *y*, –1 + *z*)
F(5)	0	0.6272	¼	¾	0.8772	0	F(1), (1 – *x*, 1 – *y*, –*z*)

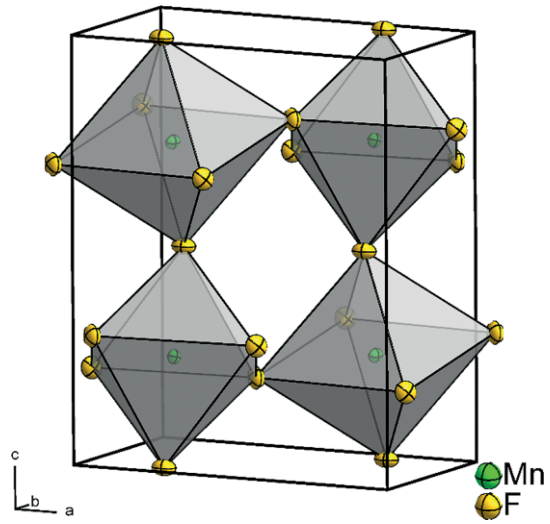

Figure 2. Crystal structure of MnF_3. The displacement ellipsoids are shown at the 70 % probability level at 183 K.

Table 4. Selected interatomic distances *d* and their multiplicities *m* for MnF_3.

Atom 1	Atom 2	*m*	*d* /Å
Mn(1)	F(2)	2	1.8124(6)
	F(1)	2	1.9037(4)
	F(2)	2	2.0806(6)

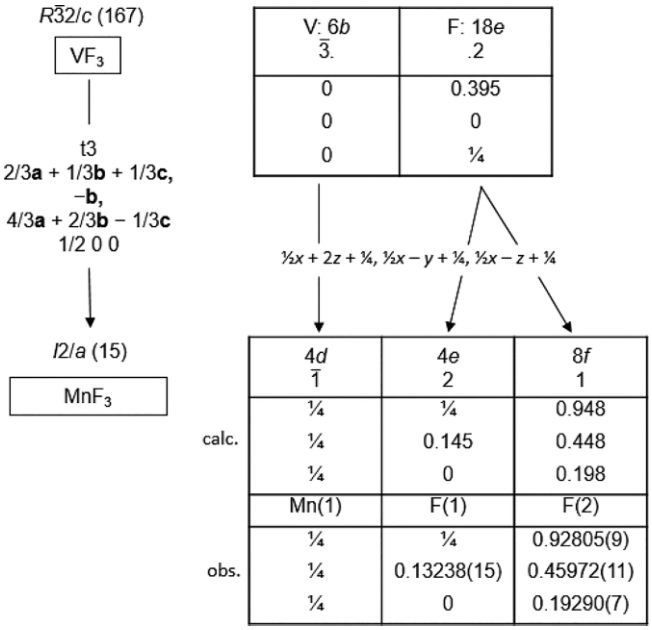

Figure 3. Bärnighausen-tree which shows the relationship between the VF_3 structure and the MnF_3 structure. Data for VF_3 are from the literature.[10]

for the manganese atom. Thus, the assignment of the oxidation states –1 and +3, respectively, is supported.

We also carried out quantum chemical calculations at the DFT-PBE0/TZVP level of theory (for details see Experimental Section) for the crystal structure and obtained optimized lattice parameters $a = 5.558$, $b = 5.075$, $c = 7.320$ Å, $\beta = 92.58°$, $V = 206.26$ Å^3, $Z = 4$ ($T = 0$ K). The calculated lattice parameters agree well with the experimentally obtained ones and are only slightly larger, which leads to a volume increase of the unit cell of circa 4 %. The calculated atomic positions are given in Table 6 and deviate only slightly from the experimentally observed positions (see Table 2). The calculated Mn–F distances are 1.82, 1.92, 2.11 Å and agree well with the respective, experimentally observed atom distances of 1.8124(6), 1.9037(4), 2.0806(6) Å.

Powder X-ray Diffraction

The powdered sample was transferred into a silica-capillary and a powder X-ray diffraction pattern was recorded at 293 K. The pattern is shown in Figure 4 and only small impurities of boron nitride, from the crucible that contains the Pt capsule, could be detected. The Rietveld refinement shows that at room temperature the same crystal structure is present as at 183 K. The refinement details are given in Table 7 and the refined atom positions and bond lengths are available from Table 8 and Table 9.

Vibrational Spectroscopy

The experimentally obtained and theoretically calculated vibrational spectra are in good agreement. The recorded IR spectrum is not of the highest quality due to the small amount of the sample. The broad band at 546 cm^{-1} can be interpreted as an overlap of the two calculated bands at 592 and 515 cm^{-1} (Figure 5). In the measured Raman spectrum, all bands except those at 200 and 175 cm^{-1} agree well with the calculated one (Figure 6). These two bands overlap and show a broad band in the recorded spectrum. The band assignment is given in Table 10.

Conclusions

Ruby red crystals of MnF_3 were synthesized by a high-pressure/high-temperature method by decomposition of MnF_4.

Table 5. Motifs of mutual adjunction, effective coordination numbers (ECoN), and mean fictive ionic radii (MEFIR) (in Å) and CHARDI for MnF_3.

	F(1)	F(2)	C. N.	ECoN	MEFIR	CHARDI
Mn(1)	2/2 1.904	4/2 1.812, 2.081	6	5.32	0.769	+3.00
C. N.	2	2				
ECoN	2.00	1.65				
MEFIR	1.128	1.114				
CHARDI	–1.077	–0.961				

Table 6. Quantum chemically calculated atom positions for MnF_3.

Atom	Position	*x*	*y*	*z*
Mn(1)	4*d*	1/4	1/4	1/4
F(1)	4*e*	1/4	0.1387	0
F(2)	8*f*	0.9275	0.4625	0.1953

MnF_3 crystallizes in the monoclinic space group *I*2/*a* (no.15) with a = 5.4964(11), b = 5.0084(10), c = 7.2411(14) Å, β = 93.00(3)°, V = 199.06(7) Å^3, Z = 4, *mS*16, T = 183(2) K. Thus, the crystal structure of MnF_3 is herewith corrected and its symmetry relation related by a direct group-subgroup transition to the VF_3 structure-type is shown. We performed quantum chemical calculations on the crystal structure to allow for the assignment of bands in the recorded IR and Raman spectra.

Experimental Section

Synthesis of MnF_4: The MnF_4 that was used to obtain single crystals of MnF_3 was synthesized by the direct fluorination of MnF_2 in a stream of 10 % (v/v) F_2 (Solvay, > 99.0 %) in argon (5.0, Praxair) with a flow of approximately 2 mL·min^{-1}.[13,14] At the synthesis temperature of 550 °C, MnF_4 sublimed and was collected at a water-cooled, gold-coated cooling finger that was made out of Monel. The greyish product was transferred under a stream of argon (5.0, Praxair) into a dried FEP transfer vessel and stored in a PTFE vessel inside a glove-box (MBraun).

Synthesis of MnF_3: Single crystals of MnF_3 were synthesized via a high-pressure/high-temperature approach. As starting material, MnF_4 was used and transferred into a platinum capsule (99.95 %, Ögussa, Vienna, Austria). Subsequently, the platinum capsule was inserted into a boron nitride crucible (Henze Boron Nitride Products AG, Lauben, Germany), which was placed into an 14/8 assembly. Handling of the starting material, as well as the preparation of the assembly was carried out under argon atmosphere (MBraun Inertgas-System GmbH, Germany). The 14/8 assembly was placed in the center of eight tungsten carbide cubes (Hawedia, Marklkofen, Germany), which transferred the pressure from a 1000 t multi-anvil press utilizing a Walker-type module (Max Voggenreiter GmbH, Mainleus, Germany) to the sample. A detailed description of the set-up and the preparation of the assembly is available in the literature.[15–17] MnF_4 was compressed to 5.5 GPa within 140 min and kept at that pressure during the heating program. Within 10 min, the sample was heated to 500 °C, kept at that temperature for 30 min, and subsequently cooled to 200 °C within 60 min. Afterwards the heating was switched off and the sample was quenched to room temperature. Upon completion of the heating program, the sample was decompressed within 330 min. Recovery of the sample was carried out in an inert gas atmosphere.

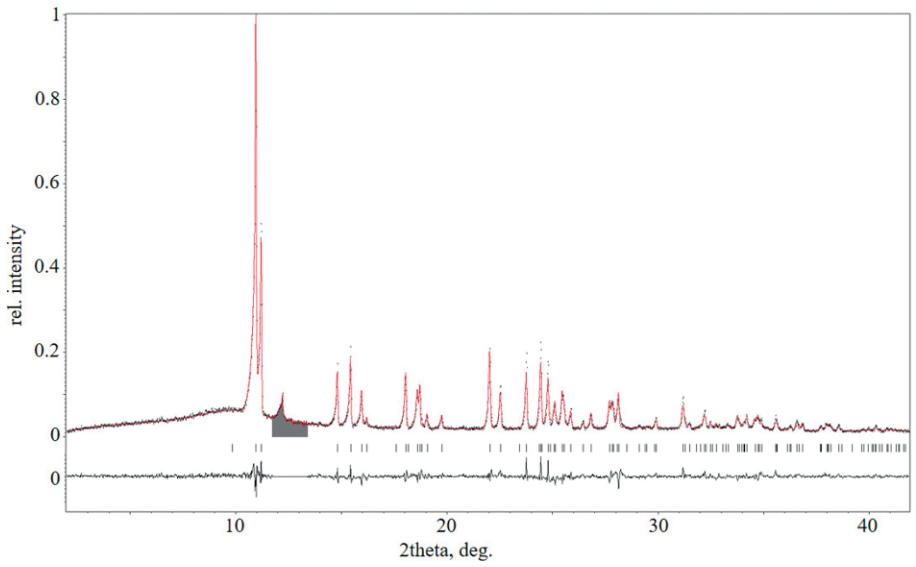

Figure 4. Observed (black) and calculated powder X-ray pattern (red) of MnF_3 after Rietveld refinement. The calculated reflection positions are indicated by the vertical bars below the pattern. The curve at the bottom represents the difference between the observed and the calculated intensities. The greyish region was excluded due to impurities of boron nitride from the crucible. R_p = 7.17, R_{wp} = 9.56 (not background corrected R values), S = 1.38.

Table 7. Selected crystallographic data and details of the Rietveld refinement of MnF_3.

	MnF_3
Molar mass /g·mol^{-1}	111.94
Space group (no.)	*I*2/*a* (15)
a /Å	5.5017(5)
b /Å	5.0270(5)
c /Å	7.2619(7)
β /°	92.814(8)
V /Å^3	200.60(3)
Z	4
Pearson symbol	*mS*16
$\rho_{calcd.}$ /g·cm^{-3}	3.7062
Color of the powder	ruby red
T /K	293
λ /Å	0.7093 (Mo-$K_{\alpha1}$)
$2\theta_{min}$, $2\theta_{max}$, $2\theta_{step}$ / °	2.000, 41.885, 0.015
No. of data points	2660
No. of parameters	17
No. of restrains	0
No. of constrains	0
Peak shape function	Pseudo-Voigt
Background	manual
S	1.38
R_p, R_{wp}	7.17, 9.56
cR_p, cR_{wp} [a]	20.24, 19.82
$R_B(I)$	8.66
$\Delta\rho_{max}$, $\Delta\rho_{min}$ /e·Å^{-3}	0.43, –0.93

a) Background-corrected R-factors.

Table 8. Atomic coordinates and isotropic displacement parameters U_{iso} for MnF_3 from Rietveld refinement at 293 K.

Atom	Position	*x*	*y*	*z*	U_{iso} /Å^2
Mn(1)	4*d*	1/4	1/4	1/4	0.0460(14)
F(1)	4*e*	1/4	0.136(2)	0	0.044(4)
F(2)	8*f*	0.9278(16)	0.4620(17)	0.1943(12)	0.039(3)

Table 9. Selected interatomic distances *d* and their multiplicities *m* for MnF_3 from Rietveld refinement at 293 K.

Atom 1	Atom 2	*m*	*d* /Å
Mn(1)	F(2)	2	1.804(9)
	F(1)	2	1.904(4)
	F(2)	2	2.091(9)

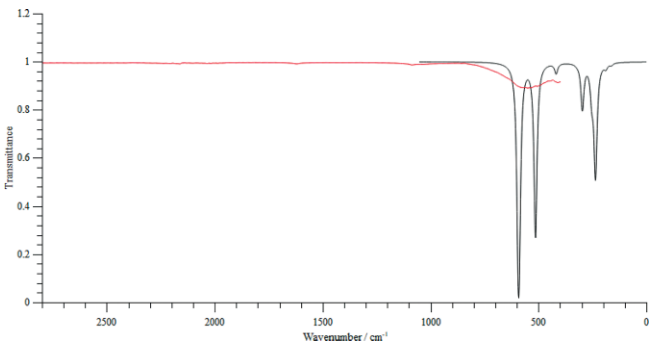

Figure 5. Experimentally observed (red) and calculated (black) IR spectra of MnF_3. Due to instrument limitations, no IR bands below 400 cm^{-1} were recorded.

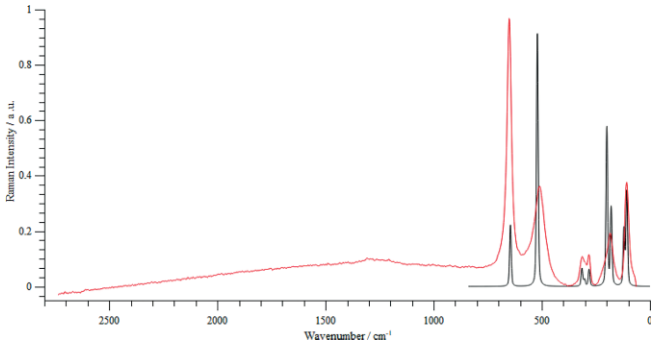

Figure 6. Experimentally observed (red) and calculated (black) Raman spectra of MnF_3.

Single Crystal X-ray Diffraction: A single crystal of the sample was isolated under perfluoropolyalkylether using a polarization microscope. The crystal was mounted onto a Bruker D8 Quest diffractometer (BRUKER, Billerica, USA). The measurement was carried out at 183(2) K and a molybdenum radiation source (Mo-K_α radiation, λ = 0.7107 Å) was used. The diffractometer is equipped with a Photon 100 detector and an Incoatec microfocus X-ray tube (Incoatec, Geesthacht, Germany). Intensity data was corrected by a multi-scan absorption correction using SADABS 2014/5.[18] The structure was solved with Direct Methods in SHELXS-86 which was included in WINGX-2013[19], refined against F^2 (SHELXL-2014/7) and graphics were made with Diamond.[20–23]

Powder X-ray Diffraction: The powder sample was filled into a 0.3 mm silica capillary and measured in Debye Scherrer mode. For the analysis, a Stoe Stadi P diffractometer (Stoe, Darmstadt, Germany) was used in transmission geometry. The diffractometer operates with Mo-$K_{\alpha1}$ radiation (λ = 0.7093 Å) and a Ge(111) primary beam monochromator. Diffraction data were recorded in a range of 2.0 to 40.4° 2θ with a step size of 0.015° by a Mythen 2 DCS4 detector. The Rietveld refinement was performed with Jana2006.[24]

Crystallographic data (excluding structure factors) for the structure in this paper have been deposited with the Cambridge Crystallographic Data Centre, CCDC, 12 Union Road, Cambridge CB21EZ, UK. Copies of the data can be obtained free of charge on quoting the depository number CCDC-1979304 and CCDC-1979305 (Fax: +44-1223-336-033; E-Mail: deposit@ccdc.cam.ac.uk, http://www.ccdc.cam.ac.uk).

IR Spectroscopy: Infrared spectra were measured on a Bruker Alpha Platinum FT-IR spectrometer using the ATR Diamond module with a resolution of 4 cm^{-1}. The spectrometer was located inside a glovebox under argon (5.0, Praxair) atmosphere. For data collection, the OPUS 7.2 software was used.[25]

Raman Spectroscopy: The Raman spectrum was recorded with a Confocal Raman Microscope S+I MonoVista CRS+, using the 633 nm excitation line of an integrated diode laser (resolution $<$ 1 cm^{-1}; range 60 to 2700 cm^{-1}).[26] The sample was measured inside a glass vessel.

Quantumchemical Calculations: The structural properties of MnF_3 were investigated using the CRYSTAL17 program package.[27] Both, the atomic positions as well as the lattice parameters were fully optimized using the PBE0 hybrid density functional method.[28,29] Triple-zeta-valence + polarization (TZVP) level basis sets derived from the molecular Karlsruhe basis sets,[30] were applied (see supporting information for full basis set details).[31,32] For spin-polarized calculations, an antiferromagnetic ordering of Mn^{III} atom spins was derived by low-

Table 10. Assignment of the vibrational modes of MnF_3. Frequencies in cm^{-1} units.

IR exp. [a]	IR calcd.	Raman exp.	Raman calcd.	Symmetry [b]	Approximate assignment of the mode [c]
		651	645	A_g	Totally symmetric Mn–F stretching within each MnF_6 unit
546 (br)	594			A_u	Asymmetric Mn–F(1) stretching, opposite F(1) atoms in *anti*-phase
	588			A_u	Asymmetric Mn–F(1) stretching, opposite F(1) atoms in *anti*-phase
	514			A_u	Asymmetric Mn–F(2) stretching, opposite F(2) atoms in *anti*-phase
		511	520	A_g	Symmetric Mn–F(1) stretching, opposite F(1) atoms in the same phase
414 (low int.)	418			A_u	Asymmetric Mn–F(2) stretching, Mn atoms in the same phase
		315	314	A_g	Symmetric F(1)–Mn–F(2) scissoring of neighboring octahedra
	322			A_u	Asymmetric F(1)–Mn–F(2) scissoring of neighboring octahedra
		299	302	A_g	Symmetric F(1)–Mn–F(1) scissoring coupled with Mn–F(2) stretching
	297			A_u	Deformation of the MnF_6 octahedra
		282	281	A_g	
	253			A_u	
	236			A_u	
	235			A_u	
	226			A_u	
		shoulder	199	A_g	
	188			A_u	
		184	179	A_g	
	162			A_u	
		–	120	A_g	
		107	107	A_g	

a) No experimentally observed IR bands below 400 cm^{-1} are given due to the limitation of the instrument. b) Calculation was carried out in space group $P\bar{1}$ to describe the antiferromagnetic ground state (see computational details). c) Due to the three-dimensional linking of the MnF_6 units, the vibrational modes are rather complex and only approximate assignments are given. Below 300 cm^{-1}, the bands are lattice vibrations.

ering the symmetry of the structure to $P\bar{1}$ so that neighboring manganese atoms have spins of the opposite sign. The reciprocal space was sampled using an $8 \times 8 \times 8$ Monkhorst-Pack-type *k*-point grid.[33] For the evaluation of the Coulomb and exchange integrals (TOLINTEG), tight tolerance factors of 8, 8, 8, 8, and 16 were used. Default optimization convergence thresholds and DFT integration grids were applied in all calculations. The harmonic vibrational frequencies,[34,35] Raman, and IR intensities,[36,37] were obtained by using the computational schemes implemented in CRYSTAL. A Lorentzian line shape with FWHM of 16 cm^{-1} was used for the calculation of the IR spectrum. The pseudo-Voigt (Gaussian:Lorentzian = 50:50) line shape with FWHM of 8 cm^{-1} was used for the calculation of the Raman spectrum. The peak assignment was carried out by visual inspection of the normal modes in the Jmol program package [38]

For charge distribution methods (CHARDI), the program CHARDI2015[39–41] was used. As input parameters we used the single crystal structure data determined in this paper. For calculation of the Madelung constant and MAPLE values, the program MAPLE 4.0 was used.[42–46] As a starting value for the fluorine atom radius 1.145 Å was chosen, as published by Shannon.[47] The given ECoN and MEFIR values are also calculated with CHARDI2015.[39–41]

Acknowledgements

We want to thank the DFG for funding, *H. L. Deubner* for Raman measurement, and *Solvay* for kind donations of F_2.

Keywords: Fluorides; Manganese; Structure elucidation; Redetermination; Quantum chemical calculations

References

[1] J. Nicklès, *C. R. Hebd. Seances Acad. Sci.* **1867**, *65*, 107–111.
[2] H. Moissan, *C. R. Hebd. Seances Acad. Sci.* **1900**, *130*, 622–627.
[3] H. von Wartenberg, *Z. Anorg. Allg. Chem.* **1940**, *244*, 337–347.
[4] Georg Brauer, *Handbuch Der Präparativen Anorganischen Chemie*, Ferdinand Enke Verlag, Stuttgart, **1975**.
[5] M. A. Hepworth, K. H. Jack, *Acta Crystallogr.* **1957**, *10*, 345–351.
[6] M. A. Hepworth, K. H. Jack, *Nature* **1957**, *179–180*, 211–212.
[7] F. Schrötter, B. G. Müller, *Z. Anorg. Allg. Chem.* **1993**, *619*, 1426–1430.
[8] F. Kraus, S. I. Ivlev, J. Bandemehr, M. Sachs, C. Pietzonka, M. Conrad, M. Serafin, B. G. Müller, *Z. Anorg. Allg. Chem.* **2020**, *submitted for publication*.
[9] K. O. Christe, *Inorg. Chem.* **1986**, *25*, 3721–3722.
[10] K. H. Jack, V. Gutmann, *Acta Crystallogr.* **1951**, *4*, 246–249.
[11] M. Molinier, W. Massa, S. Khairoun, A. Tressaud, J. L. Soubeyroux, *Z. Naturforsch. B: J. Chem. Sci.* **1991**, *46*, 1669–1673.
[12] T. D. Humphries, D. A. Sheppard, M. R. Rowles, M. V. Sofianos, C. E. Buckley, *J. Mater. Chem. A* **2016**, *4*, 12170–12178.
[13] R. Hoppe, W. Dähne, W. Klemm, *Naturwissenschaften* **1961**, *48*, 429–429.
[14] R. Hoppe, W. Dähne, W. Klemm, *Justus Liebigs Ann. Chem.* **1962**, *658*, 1–5.
[15] H. Huppertz, *Z. Kristallogr., Cryst. Mater.* **2004**, *219*, 330–338.
[16] D. Walker, M. A. Carpenter, C. M. Hitch, *Am. Mineral.* **1990**, *75*, 1020–1028.
[17] D. Walker, *Am. Mineral.* **1991**, *76*, 1092–1100.
[18] G. M. Sheldrick, *SADABS V2014/5*, Bruker AXY Inc., Madison, Wisconsin, USA, **2001**.
[19] L. J. Farrugia, *J. Appl. Crystallogr.* **2012**, *45*, 849–854.
[20] G. M. Sheldrick, *Acta Crystallogr., Sect. A: Found. Crystallogr.* **2008**, *64*, 112–122.
[21] G. M. Sheldrick, *Acta Crystallogr., Sect. A: Found. Adv.* **2015**, *71*, 3–8.

[22] G. M. Sheldrick, *Acta Crystallogr., Sect. C: Struct. Chem.* **2015**, *71*, 3–8.
[23] K. Brandenburg, H. Putz, *Diamond* - Crystal and Molecular Structure Visualization, Crystal Impact GbR, Bonn, **2019**.
[24] V. Petříček, M. Dušek, L. Palatinus, *Z. Kristallogr., Cryst. Mater.* **2014**, *229*, 345–352.
[25] *OPUS V7.2*, Bruker Optik GmbH, Ettlingen, Germany, **2012**.
[26] *VistaControl*, Spectroscopy And Imaging GmbH, Warstein, Germany, **2018**.
[27] R. Dovesi, A. Erba, R. Orlando, C. M. Zicovich-Wilson, B. Civalleri, L. Maschio, M. Rérat, S. Casassa, J. Baima, S. Salustro, et al., *Wiley Interdiscip. Rev.: Comput. Mol. Sci.* **2018**, e1360.
[28] J. P. Perdew, K. Burke, M. Ernzerhof, *Phys. Rev. Lett.* **1996**, *77*, 3865–3868.
[29] C. Adamo, V. Barone, *J. Chem. Phys.* **1999**, *110*, 6158–6170.
[30] F. Weigend, R. Ahlrichs, *Phys. Chem. Chem. Phys.* **2005**, *7*, 3297–3305.
[31] A. J. Karttunen, T. Tynell, M. Karppinen, *J. Phys. Chem. C* **2015**, *119*, 13105–13114.
[32] J. Linnera, A. J. Karttunen, *Phys. Rev. B* **2019**, *100*, 144307.
[33] H. J. Monkhorst, J. D. Pack, *Phys. Rev. B* **1976**, *13*, 5188–5192.
[34] F. Pascale, C. M. Zicovich-Wilson, F. López Gejo, B. Civalleri, R. Orlando, R. Dovesi, *J. Comput. Chem.* **2004**, *25*, 888–897.
[35] C. M. Zicovich-Wilson, F. Pascale, C. Roetti, V. R. Saunders, R. Orlando, R. Dovesi, *J. Comput. Chem.* **2004**, *25*, 1873–1881.
[36] L. Maschio, B. Kirtman, R. Orlando, M. Rèrat, *J. Chem. Phys.* **2012**, *137*, 204113.
[37] L. Maschio, B. Kirtman, M. Rérat, R. Orlando, R. Dovesi, *J. Chem. Phys.* **2013**, *139*, 164101.
[38] Jmol: An Open-Source Java Viewer for Chemical Structures in 3D. Http://Www.J·mol.Org/, Jmol Team, **2019**.
[39] M. Nespolo, B. Guillot, *J. Appl. Crystallogr.* **2016**, *49*, 317–321.
[40] R. Hoppe, S. Voigt, H. Glaum, J. Kissel, H. P. Müller, K. Bernet, *J. Less-Common Met.* **1989**, *156*, 105–122.
[41] M. Nespolo, *Acta Crystallogr., Sect. B* **2016**, *72*, 51–66.
[42] R. Hübenthal, *MAPLE Version 4.0*, Gießen, **1993**.
[43] R. Hoppe, *Angew. Chem. Int. Ed. Engl.* **1966**, *5*, 95–106.
[44] R. Hoppe, *Angew. Chem. Int. Ed. Engl.* **1970**, *9*, 25–34.
[45] R. Hoppe, *Z. Anorg. Allg. Chem.* **1956**, *283*, 196–206.
[46] R. Hoppe, *Angew. Chem.* **1970**, *82*, 7–16.
[47] R. D. Shannon, *Acta Crystallogr., Sect. A* **1976**, *32*, 751–767.

Received: January 22, 2020
Published Online: ■

Journal of Inorganic and General Chemistry
ZAAC
Zeitschrift für anorganische und allgemeine Chemie

ARTICLE